Eur. J. Mineral.
2014, **26**, 257–265
Published online February 2014

Trinepheline and fabriesite: two new mineral species from the jadeite deposit of Tawmaw (Myanmar)

CRISTIANO FERRARIS[1,*], GIAN CARLO PARODI[1], SYLVAIN PONT[1], BENJAMIN RONDEAU[2] and JEAN-PIERRE LORAND[2]

[1] Laboratoire de Minéralogie et Cosmochimie du Muséum (LMCM), Muséum National d'Histoire Naturelle (MNHN), UMR 7202, CP 52, 61 rue Buffon, 75005 Paris, France
*Corresponding author, e-mail: ferraris@mnhn.fr
[2] Laboratoire de Planétologie et Géodynamique de Nantes, UMR 6112, Faculté des Sciences, Université de Nantes, BP 92208, 2 rue de la Houssinière, 44322 Nantes Cedex, France

Abstract: Two new mineral species, trinepheline ($NaAlSiO_4$) and fabriesite ($Na_3Al_3Si_3O_{12} \cdot 2H_2O$), are described from late-stage metamorphic veins of the jadeite deposit of Tawmaw-Hpakant (Myanmar). Both minerals and their names were approved by the IMA Commission on New Minerals and Mineral Names (IMA 2012–024 and IMA 2012–080). The name trinepheline is known in literature for the polymorphs of synthetic $NaAlSiO_4$ with a value of the *c* parameter that is three times that of nepheline. Fabriesite is named in memory of Jacques Fabriès (1932–2000), former professor of the ''Muséum National d'Histoire Naturelle'' in Paris (France). Fabriesite and trinepheline occur intimately intergrown together with nepheline, more rarely with albite and other feldspar-group phases such as banalsite and stronalsite; other associated minerals are jadeite and secondary products like natrolite and harmotome. All phases have been identified via electron backscatter diffraction (EBSD) patterns. Both fabriesite and trinepheline are pseudomorph after jadeite and occur as skeletal allotriomorphic crystals up to 15–20 μm long and 5–10 μm wide. They are white to yellowish in hand specimen, colourless in thin section; the streak is white and the lustre appears vitreous to greasy; they are non-fluorescent; Mohs' hardness is 5–5½. Empirical formulae (EMPA analysis) are very close to the ideal compositions with traces of Ca and K for trinepheline, and of Ca, K, Ba, Mg, Fe, and Mn for fabriesite. Calculated densities are 2.642 g cm^{-3} for trinepheline (space group $P6_1$, $a = 9.995$ Å, $c = 24.797$ Å) and 2.386 g cm^{-3} for fabriesite (space group $Pna2_1$, $a = 16.426$ Å, $b = 15.014$ Å, $c = 5.223$ Å), respectively. The strongest five lines in the calculated X-ray powder diffraction patterns [*d* (Å) (*I*)(*hkl*)] are: 3.163(100)(122), 3.834(81)(023), 4.133(49)(006), 3.272(40)(120) and 2.403(31)(127) for trinepheline; 3.41(100)(240), 4.41(77)(201), 2.97(70)(421), 2.61(40)(002) and 8.21(36)(200) for fabriesite.

Key-words: trinepheline, fabriesite, EBSD, new mineral, Tawmaw (Myanmar), nepheline, sodium aluminium silicate.

1. Introduction

Few localities in the world are as singular as the jadeite mines of Tawmaw-Hpakant in north Myanmar. These deposits have long been shrouded in mystery although they are the primary working deposits for *jade*, the most prized gem from the Far East and worldwide exceeded in price only by diamond. Historically, the term *jade* was applied to any of a number of ornamental materials that could be carved, in particular to *nephrite*, a variety of the tremolite–actinolite amphibole series with general formula $[\square(Ca_2)(Mg, Fe^{2+})_5Si_8O_{22}(OH)_2]$. The green material found in Myanmar proved to be composed primarily of a different mineral, a pyroxene, named jadeite $[Na(Al,Fe^{3+})Si_2O_6]$ (Damour, 1863; Knight & Price, 2008).

The jadeitite, a rock made up almost entirely of jadeitic pyroxene, is found in few locations worldwide (*e.g.* Tsujimori & Harlow, 2012). Besides the Tawmaw-Hpakant, the world largest and most important jadeitite (jade) deposit are: the middle Motagua Valley in Guatemala (McBirney *et al.*, 1967; Harlow, 1994; Seitz *et al.*, 2001; Yui *et al.*, 2012), the alluvial deposits of the Itoigawa–Ohmi area in the Hida Mountains and the Chugoku Mountains, in the Wakasa, Oya and Osayama areas in central Japan (Komatsu, 1990; Miyajima *et al.*, 1999 and 2001). Less important deposits occur in western Kyushu, southern Japan (Shigeno *et al.*, 2012); along the Ketchpel River, in the Pay-Yer massif, Polar Urals (Morkovkina, 1960) and along the Yenisey and Kantegir rivers, in the Borus Mountains, West Sayan–Khakassia, Russia (Dobretsov, 1963); in Itmurundy, Near-Balkhash Region, in Kazakhstan (Dobretsov & Ponomareva, 1965); along Clear Creek in the New Idria serpentinite body, in San Benito County, California (Coleman, 1961); and more recent findings in the Caribbean (Dominican Republic, *e.g.* Schertl *et al.*, 2012; eastern Cuba, *e.g.* Cárdenas-Parraga *et al.*, 2012).

DOI: 10.1127/0935-1221/2014/0026-2348
0935-1221/14/0026-2348 $ 4.05

Common to all these deposits is that jadeitite occurs in form of lenses, pods and veins or tectonic blocks within a serpentinized ultramafic matrix such as dunites (Harlow, 1994; Okay, 1997), associated to eclogites and blueschists (*e.g.* Harlow, 1994; Shi *et al.*, 2001) as a consequence of subduction to transpression tectonic events (Harlow & Sorensen, 2005). Due to their often common vein-like texture, which implies a possible metasomatic origin, jadeitites are important sources as petrological recorders of the fluid history of a subduction environment (Harlow & Sorensen, 2005; see Harlow *et al.*, 2012).

In this paper we present the study of two new mineral species, trinepheline and fabriesite, discovered within late-stage metamorphic veins of the jadeite deposit of Tawmaw-Hpakant (Myanmar). Both minerals and their names were approved by the IMA Commission on New Minerals and Mineral Names (IMA 2012–024 and IMA 2012–080). The name trinepheline is known in the literature for the polymorphs of the synthetic compound $NaAlSiO_4$ with a value of the *c* parameter that is three times that of nepheline (Brown *et al.*, 1972; Klaska, 1974; Yamada *et al.*, 1983; Selker *et al.*, 1985; Kahlenberg & Böhm, 1998; Vulić *et al.*, 2008, 2013).

Fabriesite is named in memory of Jacques Fabriès (1932–2000), an outstanding professor of Mineralogy at the Muséum National d'Histoire Naturelle (MNHN) in Paris (France). Fabriès occupied the chair of Mineralogy from 1969 until 1998; from 1990 to 1994 he was also the MNHN director. His work was dedicated to demonstrating the intimate relationship between the petrographic and mineralogical worlds as well as to the recognition that crystallography deserves a fundamental role within the so-called ''geological world''. He was president of the ''Société Française de Minéralogie et de Cristallographie'' (SFMC) in 1987.

Type material is deposited with the Mineralogical Collection of the MNHN, catalogue number MNHN-212.001.

2. Sample description and geological setting

Both trinepheline and fabriesite were discovered within a polished section of a nephelinitic-albitic jadeitite sample from the jadeite deposit of Tawmaw-Hpakant Jade Tract, Hpakant Township, Mohnyin District, Kachin State, Myanmar. The section is all what is left of the original sample (catalogue number 105-S of the petrologic collection of endogenous rocks of the MNHN). The 1.5 mm thick polished section entered the MNHN between 1913 and 1914 together with other rock samples sent by Mr Max Bauer to Prof. Alfred Lacroix (Lacroix, 1928; 1930, and references therein), as testified by both original sample labels and whole-rock chemical analyses present within the archives of the Laboratoire de Minéralogie et Cosmochimie du Muséum (LMCM) of the MNHN.

In the nephelinitic-albitic jadeitite sample, fabriesite and trinepheline occur intimately intergrown with nepheline, more rarely with albite (Fig. 1) and other feldspar-group phases such as banalsite and stronalsite. Other associated hydrous minerals such as natrolite and harmotome occur as late-stage phases (Shi *et al.*, 2012).

The jadeitite crops out across the western part of the Sagaing Fault Zone within the central Myanmar central basin, in the Phar Kant jade mining area. The deposit of Tawmaw is about 8 kilometres NNW of Hpakant village of the Mohnyin District area in the Kachin state and is part of an ophiolitic complex (latitude 25° 68' N, longitude 96° 26' E; see also figure 1 of Shi *et al.*, 2010). The ophiolitic complex belongs to the Indo-Burma Range located east of the subduction zone, where oceanic crust of the Indian plate was subducted beneath the Burmese platelet. The transform-fault zone environment of this ophiolitic complex, together with tectonic slices of glaucophane-bearing, high-pressure metamorphic rocks, results from both collision and subduction processes between the Indian and Asian tectonic plates (Swe, 1981; Mitchell, 1993; Hall, 2002; Vigny *et al.*, 2003; Shi *et al.*, 2008).

The jadeite mines of Tawmaw-Hpakant region are characterized by bodies of serpentinized peridotite surrounded

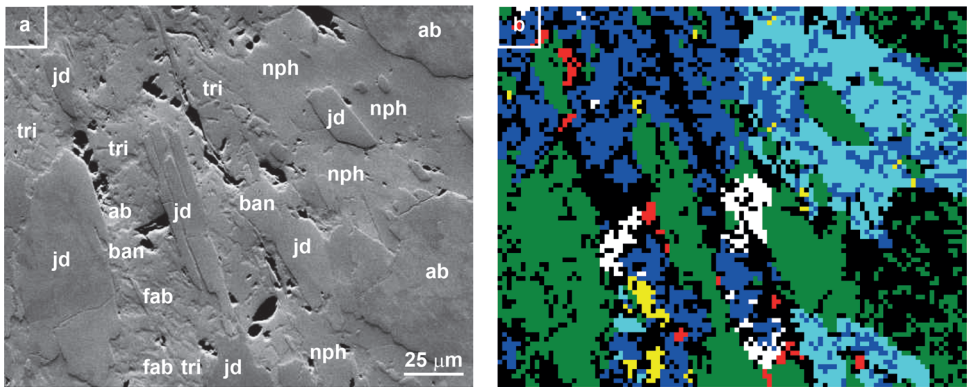

Fig. 1. (a) Secondary-electron (SE) image and (b) the corresponding EBSD elemental and crystal-structure reconstructed map showing the presence of fabriesite (fab - yellow) occurring as intergrowths together with nepheline (nph - cyan), natrolite (red), banalsite (ban - white) and trinepheline (tri - blue) after jadeite (jd - green) and albite (ab + holes – black). In the SE image, areas corresponding to fabriesite and other zeolitic products are visibly more damaged by sample surface polishing compared to nepheline, jadeite and albite.

by metamorphic schists and plutonic rocks such as granites and monzonites (Bender, 1983; Shi *et al.*, 2012). Jadeite formed independently of the intrusive bodies by crystallization from hydrous fluids (derived by dewatering of the subducted Indian plate) that rose along fractures in the serpentinized peridotite at relatively high-pressure/low-temperature conditions. This was related to the Tertiary formation of the Himalaya by Bender (1983), but sensitive high-resolution ion microprobe (SHRIMP) dating of jadeitite zircon reveals Mid- and Late-Jurassic ages (Shi *et al.*, 2008), relating jadeitite formation to subduction rather than collision stages. Fluids that form in these special conditions are generally saturated with respect to sodium alumino-silicate like jadeite at higher pressure, albite and nepheline at lower pressure.

Lacroix (1930) describes the Tawmaw dyke as an assemblage of jadeitite *s.s.* together with albitite and amphibolite. These rocks are not recognized as distinct geological entities but represent a chemical zonation within the same ''jadeitite'' dyke; the Na-rich pyroxene volumes occupies the central portion of the dyke surrounded, from the core to the outer parts (*i.e.* contacts with the embedding serpentinite), by albitite and amphibolite, respectively. Within the jadeite *s.s.*, albite areas up to 1 mm across are partly replaced by late-stage mesolite. Some portions of the jadeitite partly show a transition to albite ± nepheline and locally are crosscut by thin late-stage albite veins, which are commonly less than 5 mm wide (Harlow *et al.*, 2007; Shi *et al.*, 2008) even if, rarely, centimetric ones have been reported (figure 2f in Shi *et al.*, 2012). Within these veins, poecilitic crystals of nepheline embed allotriomorphic jadeite partly corroded together with albite, natrolite, banalsite, stronalsite, harmotome and the two new species here described, trinepheline and fabriesite.

The precise metamorphic peak conditions for the jadeitite bodies in Tawmaw are still matter of debate (*cf.* Shi *et al.*, 2012 and references therein) with a pressure range comprised between 1 and 1.5 GPa and temperatures above 300°C and lower than 500°C. Shi *et al.* (2012) also suggest that, following this peak event, a more articulated late-stage one, where nephelinitic-albitic jadeitites may have been equilibrated at somewhat lower *T* and *P*, is characterized by feldspar-group products of both series celsian–hyalophane and banalsite–stronalsite and by zeolitic products.

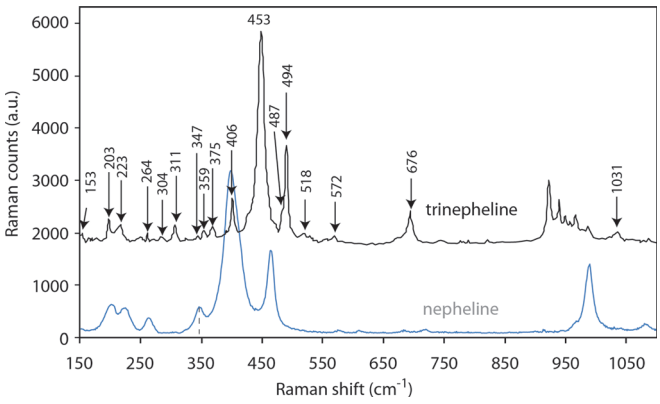

Fig. 2. The Raman spectrum of trinepheline compared to that of nepheline. Comparison of the two spectra clearly shows the minerals to be different. The nepheline reference Raman spectrum $(Na_{0.77}K_{0.23})AlSiO_4$ (non-oriented sample; 514 nm laser) is from RRUFF database (Downs, 2006); all Raman data together with chemical analyses and X-ray data for this phase are available on the RRUFF website (http://rruff.info/) under RRUFF ID: R040025.

3. Analytical methods

Wavelength dispersive X-ray spectroscopy (WDS) analyses were performed with an electron microprobe CAMECA SX100 (Service d'Analyse Microsonde Camparis - Université Pierre et Marie Curie, Paris 6) at an accelerating voltage of 15kV for a probe current intensity of 10 nA and a probe size of 5 µm.

The crystallographic characterization of the new mineral phases was done by electron backscatter diffraction (EBSD) obtained using the dedicated CamScan X500FE CrystalProbe device of the ''Laboratoire de Géosciences'' in Montpellier (France) (Université Montpellier 2). The samples were not coated with carbon to lower absorption effects. The experimental EBSD patterns were automatically indexed by comparison with simulated patterns based on Crystallographic Information Files (CIF) extracted from the inorganic crystal structure database (ICSD-Fiz Karlsruhe) using the CHANNEL5 software (HKL-Oxford Instruments). Only the fitting solutions with a Mean Angular Deviation (MAD) lower than 1° were considered.

The Raman spectra were acquired using a Renishaw inVia spectrometer equipped with a 1800 l/mm grating at the ''Centre de Recherche sur la Conservation des Collections'' (CRCC) of the MNHN. The excitation source was provided by a laser with a wavelength of 532 nm and a power of 50 mW. The working conditions were an exposure time of 10 s and a laser power of 10 % on a Raman shift ranging from 100 to 4000 cm^{-1}.

All the backscattered-electron pictures and the energy-dispersive X-ray spectroscopy (EDS) analyses were obtained at the MNHN, using a scanning electron microscope Tescan VEGAII LSU coupled with a Bruker XFlash EDS SDD detector.

4. Results

Trinepheline (hexagonal $NaAlSiO_4$) and fabriesite ($Na_3Al_3Si_3O_{12} \cdot 2H_2O$), identified via EBSD patterns as discussed later, are pseudomorph after jadeite. Both phases generally occur as skeletal allotriomorphic crystals up to 15–20 µm long and 5–10 µm wide, respectively (Fig. 1a); pseudo-idiomorphic prismatic crystals are very rare. Within the sample, both trinepheline and fabriesite are detectable only by combining scanning electron microscopy imaging systems, microprobe analyses and EBSD

mapping techniques (Fig. 1). Secondary electron (SE) images (Fig. 1a) clearly show that these phases are softer and more sensitive to polishing-induced damage than nepheline and jadeite. Because of both the small size of the available crystals and their complex intergrowths, only some physical properties could be determined. For both phases the colour is white to yellowish in hand specimen, colourless in thin section, the streak is white and the lustre appears vitreous to greasy. The minerals are non-fluorescent and their hardness H (Mohs) is estimated between 5 and 5½ according to their behaviour during polishing in comparison to the known hardness of intergrown nepheline and natrolite. For synthetic ''nepheline hydrate I'' (NHI), corresponding to fabriesite (see below), Barrer & White (1952) report biaxial (–) character, $\alpha = 1.503$, $\beta = 1.506$, $\gamma = 1.508$, $2V$ (calc.) = 78°; the calculated mean refractive index is 1.511 that is slightly higher compared to the values measured for NHI. For synthetic trinepheline, Kahlenberg & Böhm (1998) do not report optical data; the calculated mean refractive index is 1.538 in agreement with the values reported for natural nephelines ($n_\omega = 1.529$–1.546; $n_\varepsilon = 1.526$–1.542; Nesse, 2000). Densities of 2.642 and 2.386 g cm^{-3} are calculated for trinepheline and fabriesite, respectively.

4.1. Chemical composition and Raman spectra

Microprobe analyses (Table 1) and Raman data indicate that:

- *trinepheline* is an anhydrous mineral with empirical formula (based on 4 O atoms pfu) $(Na_{0.996}Ca_{0.002}K_{0.002})Al_{1.011}Si_{0.990}O_4$ and simplified formula $NaAlSiO_4$;
- *fabriesite* (Table 2) is a hydrous phase (Fig. 3a) with empirical formula (based on 14 O atoms pfu) $(Na_{2.937}Ca_{0.030}K_{0.008}Mg_{0.007}Fe_{0.004}Ba_{0.002}Mn_{0.001})_{\sum=2.989}Al_{2.996}Si_{2.999}O_{12} \cdot 2H_{1.993}O$ and simplified formula $Na_3Al_3Si_3O_{12} \cdot nH_2O$.

Comparison of the Raman spectrum of trinepheline (Fig. 2) with that of nepheline [reference Raman spectrum $(Na_{0.77}K_{0.23})AlSiO_4$; non-oriented sample; 514 nm laser - RRUFF database (Downs, 2006)] indicates that: *i*) peaks for nepheline and trinepheline coincide in the region 150–264 cm^{-1}; *ii*) the strong peaks of trinepheline are

Table 1. Analytical data for trinepheline based on 12 analyses on four different grains.

Constituent	wt%	Range	SD	Probe standard
Na_2O	21.68	20.31–22.22	0.58	Albite
MgO	0.01	0.00–0.09	0.03	Diopside
SiO_2	41.76	41.33–42.09	0.30	Diopside
Al_2O_3	36.19	35.70–37.15	0.45	Orthoclase
K_2O	0.08	0.03–0.12	0.04	Orthoclase
CaO	0.10	0.00–0.25	0.09	Diopside
FeO	0.06	0.00–0.18	0.08	Garnet
Total	99.88			

Table 2. Analytical data for fabriesite based on 10 analyses on three different grains.

Constituent	wt%	Range	SD	Probe standard
Na_2O	19.67	18.31–20.22	0.54	Albite
MgO	0.06	0.03–0.11	0.04	Diopside
SiO_2	38.93	37.95–40.09	0.31	Diopside
Al_2O_3	33.00	32.81–33.95	0.23	Orthoclase
K_2O	0.08	0.05–0.11	0.04	Orthoclase
CaO	0.36	0.28–0.68	0.19	Diopside
FeO	0.06	0.03–0.18	0.08	Garnet
MnO	0.01	0.00–0.03	0.03	Synthetic $MnTiO_3$
BaO	0.07	0.02–0.09	0.06	Synthetic $BaSO_4$
H_2O*	7.76			
Total	100.00			

* by difference to 100 %

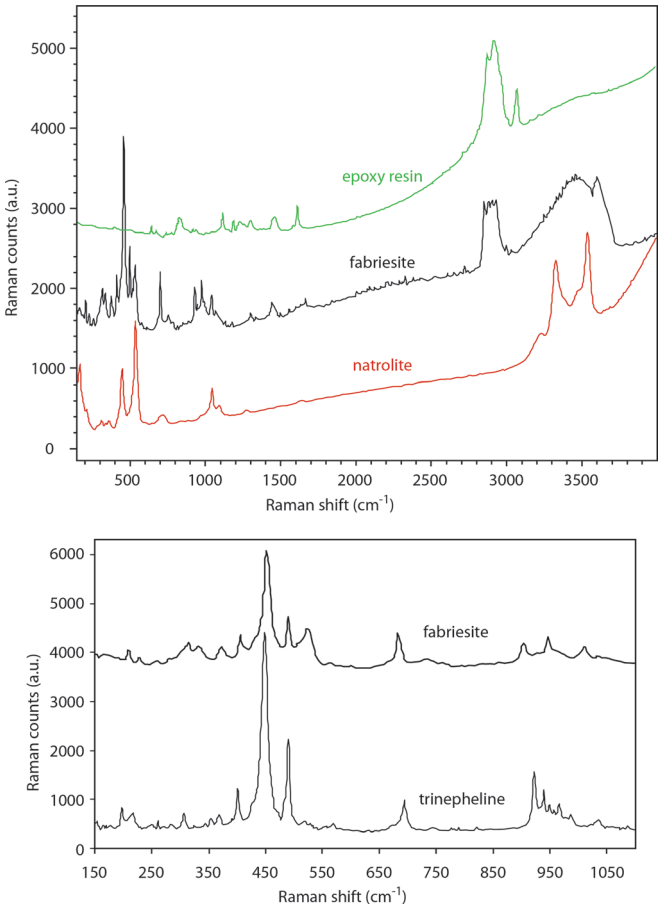

Fig. 3. **Top**: Raman spectra of fabriesite (black) compared to those of natrolite (red) and an epoxy resin present in the polished thin section. Comparison of the three spectra clearly points out the characteristics of fabriesite. Besides typical peaks at low values (< 1800 cm^{-1}) comparable to those of natrolite, fabriesite clearly shows, even if very broad compared to those of natrolite, peaks due to the presence of water centred at around 3200 and 3500 cm^{-1}. The peak centred at about 2900 cm^{-1} corresponds to a signal due to epoxy resin in the thin polished sections. **Bottom**: Raman spectra of trinepheline and fabriesite in the 150–1100 cm^{-1} range.

shifted compared to those of nepheline (406 *vs.* 347 cm^{-1}, 453 *vs.* 400 cm^{-1} and 494 *vs.* 466 cm^{-1} respectively); *iii*) the differences in the region between 926 and 1031 cm^{-1} are related to differences in intensities.

Comparison of the Raman spectrum of fabriesite with those of natrolite and trinepheline occurring in the same sample (Figs. 3a and 1b) shows that, besides peaks at low frequencies (< 1800 cm^{-1}) which are similar to those observed in natrolite and trinepheline (Fig. 3b), fabriesite is characterized by peaks centred at around 3200 and 3500 cm^{-1} due to the presence of water. The peak centred at about 2900 cm^{-1} is due to the epoxy resin (Fig. 1a).

4.2. Crystallographic data

For both trinepheline and fabriesite single-crystal X-ray diffraction studies could not be carried out because of both scarcity of material and small size of the crystals. Crystallographic information was instead obtained by single-crystal EBSD analyses.

For trinepheline, the experimental EBSD pattern (Fig. 4a) was successfully matched (MAD = 0.3°) to that calculated using the structural data of synthetic hexagonal $NaAlSiO_4$ (space group $P6_1$, $a = 9.995$ Å, $c = 24.797$ Å, $Z = 24$; ICSD 85553 - Kahlenberg & Böhm, 1998). All the other tested structures with chemical composition $NaAlSiO_4$ (Buerger *et al.*, 1946 – ICSD 36324; Brown *et al.*, 1972; Klaska, 1974; Yamada *et al.*, 1983 – ICSD 46008; Selker *et al.*, 1985; Kahlenberg & Böhm, 1998; Vulić *et al.*, 2008, 2013) were discarded because the MAD test was higher than 0.5°. Interplanar distances [*d* (Å)] and X-ray powder diffraction intensities [*I*(%)] for Cu*Kα* radiation were calculated with data of Kahlenberg & Böhm (1998) and are listed in Table 3.

The experimental EBSD pattern of fabriesite (Fig. 4b) was matched (MAD = 0.4°) to that calculated using data of synthetic orthorhombic $Na_3Al_3Si_3O_{12} \cdot 2H_2O$ [space group

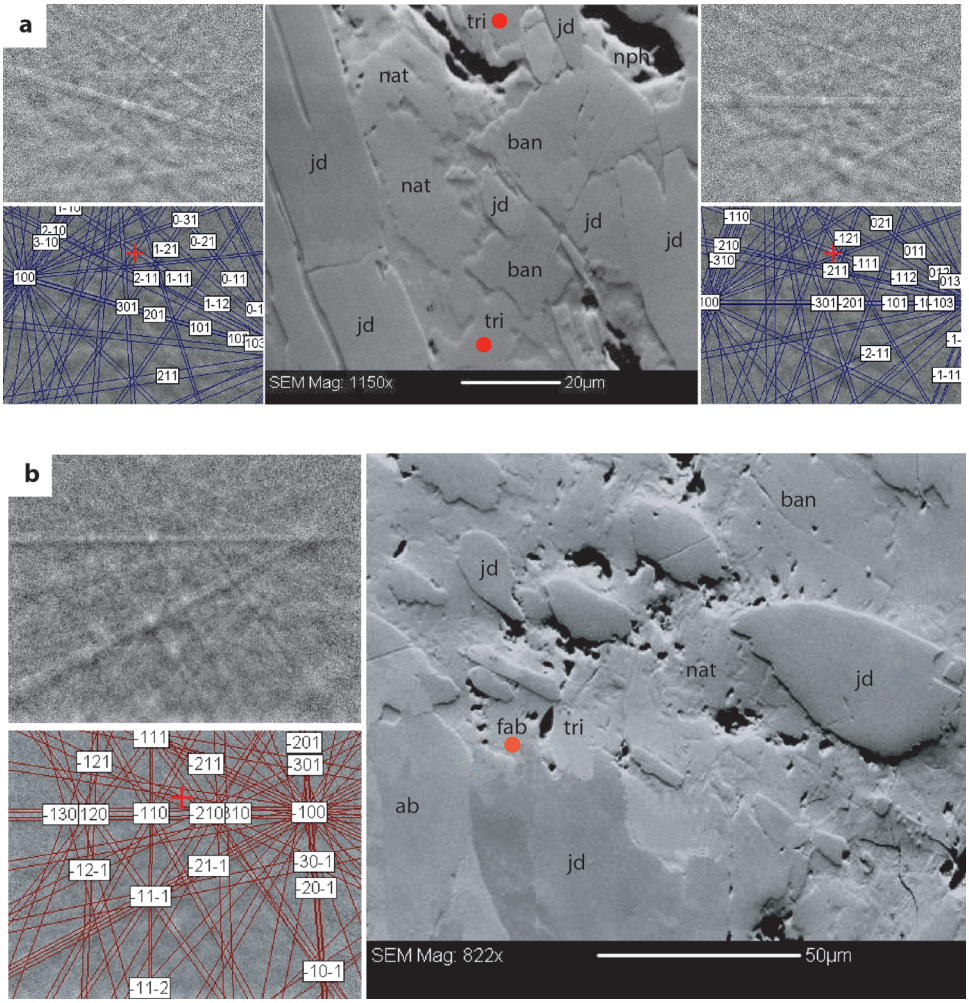

Fig. 4. (a) Secondary-electron (SE) image (centre) and trinepheline EBSD patterns (left and right top sides) collected at the red circles on the SE image (red filled circles). The left diffraction pattern corresponds to the bottom point of the SE image. Below each experimental EBSD pattern the indexing obtained using data from ICSD 85553 (Kahlenberg & Böhm, 1998) is reported; jd = jadeite, nat = natrolite, ban = banalsite, tri = trinepheline, nph = nepheline. (b) Secondary-electron image (right) and fabriesite EBSD patterns (left top) collected at the red circle on the SE image; jd = jadeite; nat = natrolite; ban = banalsite; tri = trinepheline; fab = fabriesite. Below the EBSD pattern is the indexing of the Kikuchi lines obtained using data from ICSD 201460 (Hansen & Fälth, 1982).

Table 3. Calculated X – ray powder diffraction data for trinepheline based on the structure data of Kahlenberg & Böhm (1998). The eight strongest reflections are in bold type.

h	*k*	*l*	*d* [Å]	I_{rel}
0	**2**	**0**	**4.328**	**22**
0	**0**	**6**	**4.133**	**49**
0	**2**	**3**	**3.834**	**81**
1	**2**	**0**	**3.272**	**40**
2	1	1	3.244	19
1	1	6	3.185	16
1	**2**	**2**	**3.163**	**100**
1	2	3	3.042	9
2	1	3	3.042	12
0	**2**	**6**	**2.989**	**21**
1	1	7	2.890	6
1	2	5	2.731	12
0	3	3	2.724	20
0	3	4	2.616	5
0	2	8	2.520	12
1	**2**	**7**	**2.403**	**31**
2	1	7	2.403	9
1	**3**	**0**	**2.401**	**22**
2	1	8	2.250	5
0	3	7	2.237	12
0	2	10	2.152	7
1	3	6	2.076	6
0	3	10	1.881	7
0	5	1	1.727	14
0	3	12	1.680	16
2	4	1	1.632	5
4	2	3	1.605	10
1	5	0	1.555	9
4	2	6	1.521	5
0	3	16	1.365	5

Table 4. Calculated X-ray powder-diffraction data for fabriesite based on the structure data of Hansen & Fälth (1982). The eight strongest reflections are in bold type.

h	*k*	*l*	*d* [Å]	I_{rel}
2	**0**	**0**	**8.21**	**36**
0	**2**	**0**	**7.51**	**32**
2	2	0	5.54	12
2	**0**	**1**	**4.41**	**77**
2	**4**	**0**	**3.41**	**100**
4	**2**	**1**	**2.97**	**70**
2	**4**	**1**	**2.86**	**25**
0	**0**	**2**	**2.61**	**40**
4	**4**	**1**	**2.45**	**29**
6	0	1	2.42	15
6	2	1	2.31	6
4	0	2	2.20	6
2	4	2	2.07	8
0	8	0	1.88	18
6	6	1	1.74	9
2	0	3	1.70	6
8	0	2	1.61	7
4	2	3	1.57	12
0	8	2	1.52	6
10	4	0	1.50	6
6	8	1	1.48	7
4	4	3	1.47	7
4	10	1	1.36	10
10	4	2	1.30	7
4	10	3	1.10	5

$Pna2_1$, $a = 16.426$, $b = 15.014$, $c = 5.223$, $Z = 4$; ICSD 201460 – Hansen & Fälth, 1982]. All the other tested structures with similar chemical composition (Ragimov *et al.*, 1978 – ICSD 200679; Gramlich & Meier, 1971 – ICSD 24901; Baerlocher & Barrer, 1974 – ICSD 6272; Fälth & Andersson, 1982 – ICSD 31289; Reinhardt *et al.*, 1982 – ICSD 17069; Shepelev *et al.*, 1983 ICSD – 20645; Felsche *et al.*, 1986 – ICSD 85512; Lee *et al.*, 1998 – ICSD 85620; Albert *et al.*, 1998 – ICSD 87553) were discarded because MAD was higher than 1°. Interplanar distances [*d* (Å)] and X-ray powder diffraction intensities [*I*(%)] for Cu$K\alpha$ radiation were calculated with the data of Hansen & Fälth (1982) and are listed in Table 4.

5. Discussion

5.1. Trinepheline

Synthetic Na-rich nephelines have been widely investigated for petrologic reasons as well as for their interesting properties as solid-state ionic conductors (Dollase & Thomas, 1978; Gregorkiewitz, 1984; Roth, 1985; Hippler & Böhm, 1989). The basic structure is the same as was reported by Hahn & Buerger (1955) in space group $P6_3$ for a natural nepheline sample with idealized composition $Na_6K_2Al_8Si_8O_{32}$. The complete substitution of K^+ with smaller Na^+ cations leads to the tripling of the *c* axis for pure $NaAlSiO_4$ as first reported by Jarchow *et al.* (1966) and confirmed by Kahlenberg & Böhm (1998) (Fig. 5b).

The EBSD analysis reported above clearly identify the new mineral trinepheline with the synthetic hexagonal polymorph of $NaAlSiO_4$ described by Kahlenberg & Böhm (1998) and exclude the other polymorphs mentioned in the Introduction section. As noted by the same authors, trinepheline represents a new type of stuffed tridymite structure with close relationships to other tridymite (SiO_2) derivatives: kalsilite ($KAlSiO_4$), yoshiokaite ($CaAl_2SiO_6$) and nepheline [$(Na,K)AlSiO_4$] (Palmer, 1964; Merlino, 1984).

The trinepheline crystal structure (for details refer to Kahlenberg & Böhm, 1998) is characterized by layers of typical six-membered tetrahedral rings. These rings are built up by regularly alternating AlO_4 and SiO_4 tetrahedra. The stacking of the layers along the *c* axis results in a three-dimensional network containing channels that are occupied by irregularly coordinated Na cations (Fig. 5a). The main structural difference between nepheline of idealized composition $Na_6K_2Al_8Si_8O_{32}$ (Hahn & Buerger, 1955) and trinepheline is based on the fact that excess Na in samples containing more than 6 Na apfu must be accommodated on the large alkali site. Sodium substitution involves either the collapse of the hexagonal channels, or an off-centring of Na toward the channel wall (about 0.35 Å).

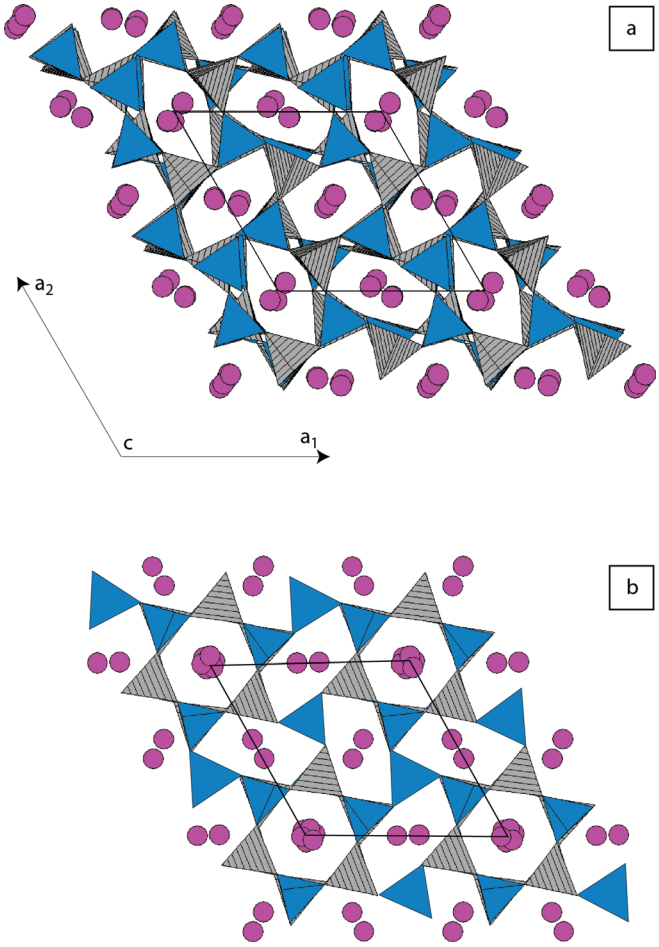

Fig. 5. (a) Crystal structure of trinepheline as viewed down *c* based on the data of Kahlenberg & Böhm (1998); purple circles indicate the Na ions. (b) Projection of the crystal structure of a Na-deficient nepheline parallel to *c*, based on the data of Hippler & Böhm (1989).

Twinning by merohedry observed on synthetic $NaAlSiO_4$ material by Kahlenberg & Böhm (1998) has not been found in natural trinepheline, which belongs to the Nickel-Strunz class 9.FA.05 (tectosilicates without zeolitic H_2O and any additional non-tetrahedral anions) and to Dana class 76.2.1.2 (tectosilicates Al-Si framework-feldspathoids and related species).

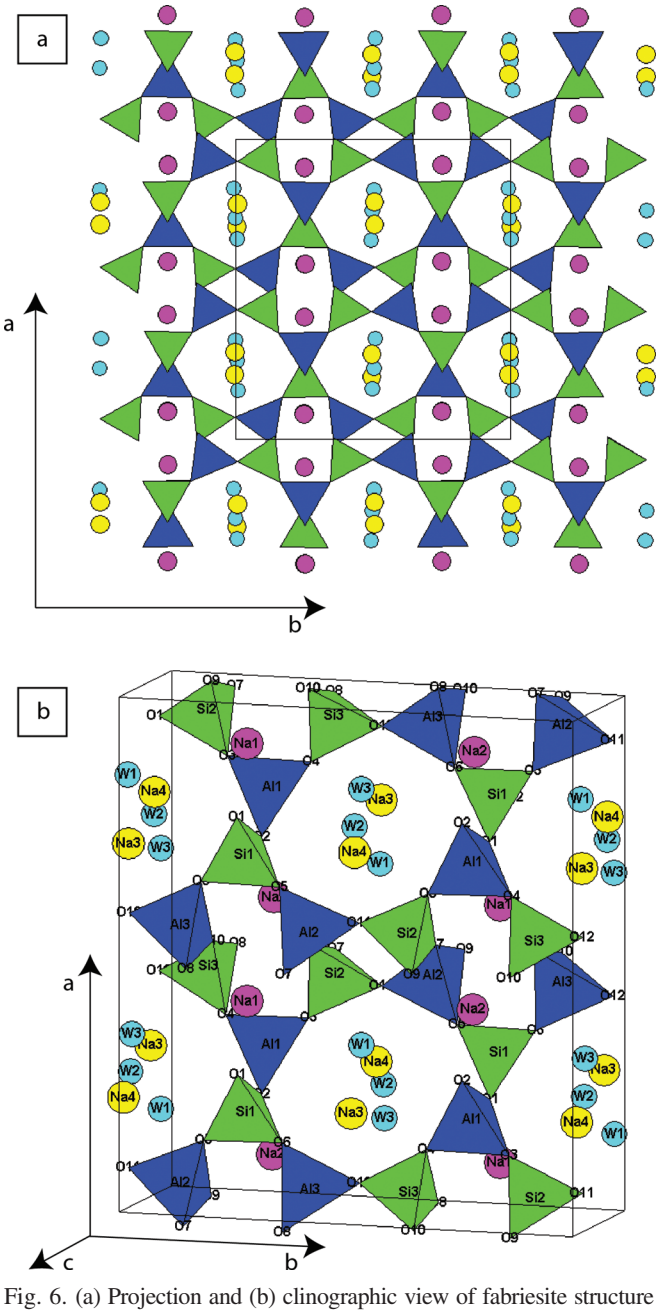

Fig. 6. (a) Projection and (b) clinographic view of fabriesite structure along *c* showing the Na ions and water molecules arrangement within tunnels developed along *c*. Based on the data of Hansen & Fälth (1982).

5.2. Fabriesite

As noted by Hansen & Fälth (1982) for the synthetic compound ''Nepheline Hydrate I'' (NHI), $Na_3Al_3Si_3O_{12} \cdot 2H_2O$, corresponding to fabriesite, the structure constitutes a link between anhydrous tectosilicates and zeolites. It consists of a set of parallel two-repeat chains with alternating single and double chains built up by a regular alternation of AlO_4 and SiO_4 tetrahedra (Fig. 6a; for details refer to fig. 2 and 3 of Hansen & Fälth, 1982 and references therein). The framework contains channels running along *c*, with elongated apertures consisting of eight-membered rings (tetrahedra). The coordination of the Na atoms is of two different types: Na(1) and Na(2) are coordinated by seven framework oxygen atoms in a distorted monocapped trigonal prism; Na(3) is instead coordinated by the oxygen atoms of three water molecules and three framework oxygen atoms forming a highly distorted octahedron (Fig. 6b).

The tetrahedral framework of fabriesite is topologically different from (but related to) the one in nepheline (tridymite). The fabriesite framework is conveniently described as consisting of alternating double and single silicate chains zig-zaging along *c*. Fabriesite belongs to Nickel-Strunz class 09.GB.05 (tectosilicates with zeolitic H_2O and chains of single connected four-membered rings), and Dana class 77.01.01.01 (tectosilicates zeolite group – analcime and related species).

5.3. Genesis

Trinepheline crystallization is related to the destabilization of jadeite crystals during a metamorphic decompression stage, according to the reaction 2 jadeite → albite + nepheline; as the reaction proceeds, trinepheline takes the place of nepheline.

The trinepheline formation at the proposed decompression metamorphic stage is related to the three following observations. Chemical analyses show that nepheline is clearly distinguishable from trinepheline as it contains up to 3.9 wt% K_2O. Differences in size clearly exist between nepheline and trinepheline (Fig. 1) (100 *vs.* 20 μm, respectively) and trinepheline occupies interstitial positions within intergrowths, in contrast to nepheline. We thus conclude that K^+ ions were no longer available because of nepheline formation, together with insufficient amounts of Si^{4+} and Al^{3+} to form more albite. Consequently, residual Na^+, Si^{4+} and Al^{3+} (in the ratio 1:1:1) converged towards the composition of trinepheline and, together with small amounts of Ba^{2+} and Sr^{2+}, to the banalsite–stronalsite crystallization.

Fabriesite formation is related to the hydration of trinepheline very likely corresponding to the late-stage metamorphic event described by Shi *et al.* (2012) and characterized by high fluid circulation.

Acknowledgements: The authors are grateful to J.R. Kienast for his suggestion to carefully analyse ''nephelines'' from Tawmaw jadeitites. We thank F. Barou and C. Nevado (Laboratoire Géosciences Montpellier) for the EBSD experiments and the samples preparation, V. Rouchon (CRCC-MNHN) for her kind support in Raman spectroscopy and for giving access to the equipment, and finally to M. Fialin for the EPMA analyses at the Service Camparis-Université Pierre et Marie Curie. The constructive criticism of two unknown referees and of the editor helped to improve the article.

References

Albert, B.R., Cheetham, A.K., Stuart, J.A., Adams, C.J. (1998): Investigations on P zeolites: synthesis, characterisation, and structure of highly-crystalline low-silica Na P. *Micropor. Mesopor. Mat.*, **21**, 133–142.

Baerlocher, C. & Barrer, R.M. (1974): The crystal structure of synthetic zeolite F. *Z. Kristallogr.*, **140**, 10–26.

Barrer, R.M. & White, E.A.D. (1952): The hydrothermal chemistry of silicates. Part II. Synthetic crystalline sodium aluminosilicates. *J. Chem. Soc.*, **286**, 1561–1571.

Bender, F. (1983): Geology of Burma. Gebrüder Bornträger, Berlin, 260 p.

Brown, W.L., Cesbron, F., Dupont, G. (1972): Trinepheline; a new synthetic modification in the nepheline group. *Z. Kristallogr.*, **136**, 468–470.

Buerger, M.J., Klein, G.E., Hamburger, G.E. (1946): Structure of nepheline. *Bull. Geol. Soc. Am.*, **57**, 1182–1183.

Cárdenas-Párraga, J., García-Casco, A., Harlow, G.E., Blanco-Quintero, I.F., Rojas Agramonte, Y., Kröner, A. (2012): Hydrothermal origin and age of jadeitites from Sierra del Convento Mélange (Eastern Cuba). *Eur. J. Mineral.*, **24**, 313–331.

Coleman, R.G. (1961): Jadeite deposits of the Clear Creek area, New Idria District, San Benito County, California. *J. Petrol.*, **2**, 225–247.

Damour, M.A. (1863): Notice et analyse sur la jade vert. Réunion de cette matière minérale à la famille des Wernerites. *C. R. Hebd. Séances Acad. Sci.*, **56**, 861–865.

Dobretsov, N.L. (1963): Mineralogy, petrography and genesis of ultrabasic rocks, jadeitites, and albitites from the Borus Mountain Range (the West Sayan). *Proc. Inst. Geol. Geophys. Acad. Sci. USSR (Siberian Branch)*, **15**, 242–316. (in Russian)

Dobretsov, N.L. & Ponomareva, L.G. (1965): Comparative characteristics of jadeite and associated rocks from Polar Ural and Near-Balkhash Region. *Trudy Inst. Geol. Geophys. Acad. Sci. USSR (Siberian Branch)*, **31**, 178–243. (in Russian)

Dollase, W.A. & Thomas, W.M. (1978): The crystal chemistry of silica-rich, alkali-deficient nepheline. *Contrib. Mineral. Petrol.*, **66**, 311–318.

Downs, R.T. (2006): The RRUFF Project: an integrated study of the chemistry, crystallography, Raman and infrared spectroscopy of minerals. *Program and Abstracts of the 19th General Meeting of the International Mineralogical Association in Kobe, Japan*. O03–13.

Fälth, L. & Andersson, S. (1982): Crystal structure of the synthetic zeolite N, $NaAlSiO_4(H_2O)_{1.3}$. *Z. Kristallogr.*, **160**, 313–316.

Felsche, J., Luger, S., Baerlocher, C. (1986): Crystal structures of the hydro-sodalite Na_6 $(AlSiO_4)_6 \cdot 8(H_2O)$ and of the anhydrous sodalite $Na_6(AlSiO_4)_6$. *Zeolites*, **6**, 367–372.

Gramlich, V. & Meier, W.M. (1971): The crystal structure of hydrated NaA: A detailed refinement of a pseudosymmetric zeolite. *Z. Kristallogr.*, **133**, 134–149.

Gregorkiewitz, M. (1984): Crystal structure and Al/Si-ordering of a synthetic nepheline. *Bull. Minéral.*, **107**, 499–507.

Hahn, T. & Buerger, M.J. (1955): The detailed structure of nepheline $KNa_3Al_4Si_4O_{16}$. *Z. Kristallogr.*, **106**, 308–338.

Hall, R. (2002): Cenozoic geological and plate tectonic evolution of SE Asia and the SW Pacific. *J. Asian Earth Sci.*, **20**, 353–434.

Hansen, S. & Fälth, L. (1982): X-ray study of the nepheline hydrate I structure. *Zeolites*, **2**, 162–166.

Harlow, G.E. (1994): Jadeitites, albitites and related rocks from the Motagua fault zone, Guatemala. *J. Metamorphic Geol.*, **12**, 49–68.

Harlow, G.E. & Sorensen, S.S. (2005): Jade (nephrite and jadeitite) and serpentinite: metasomatic connections. *Inter. Geol. Rev.*, **47**, 113–146.

Harlow, G.E., Sorensen, S.S., Sisson, V.B. (2007): Jade. In ''The geology of gem deposits'', L.A. Groat ed. Mineralogical Association of Canada, Canada, 207–254.

Harlow, G.E., Tsujimori, T., Sorensen, S.S. (2012): Introduction to the special issue 'Jadeitites: new occurrences, new data, and implications for subduction-zone fluids. *Eur. J. Mineral.*, **24**, 197–198.

Hippler, B. & Böhm, H. (1989): Structure investigations on sodium nephelines. *Z. Kristallogr.*, **187**, 39–53.

Jarchow, O., Reese, H.H., Saalfeld, H. (1966): Hydrothermalsynthesen von Zeolithen der Sodalith- und Cancrinitgruppe. *N. Jb. Miner. Mh.*, **1966**, 289–297.

Kahlenberg, V. & Böhm, H. (1998): Crystal structure of hexagonal trinepheline - A new synthetic $NaAlSiO_4$ modification. *Am. Mineral.*, **83**, 631–637.

Klaska, K.H. (1974): Strukturuntersuchungen an Tridymitabkömmlingen. Ph.D. thesis, Fachbereich Geowissenschaften, Universität Hamburg, Germany.

Knight, K.S. & Price, G.D. (2008): Powder neutron diffraction studies of clinopyroxenes: the crystal structure and thermoelastic properties of jadeite between 1.5 and 200 K. *Can. Mineral.*, **46**, 1593–1622.

Komatsu, M. (1990): Hida 'Gaien' Belt and Joetsu Belt. In ''Pre-Cretaceous Terranes of Japan'', K. Ichikawa, S. Mizutani, I. Hara, S. Hada, A. Yagi, eds. *IGCP Project*, **224**, 25–40.

Lacroix, A. (1928): Sur la genèse de la jadéite de Birmanie. *Mém. Commun. Acad. Sci*., *Paris*, séance du lundi 17 septembre 1928, 489–493.

— (1930): La jadéite de Birmanie: les roches qu'elle constitue ou qui l'accompagnent. Composition et origine. *Bull. Soc. Fr. Minéral.*, **53**, 210–254.

Lee, Y.-J., Carr, S.W., Parise, J.B. (1998): Phase transition upon K^+ ion exchange into Na-low silica X: combined NMR and synchrotron X-ray powder diffraction study. *Chem. Mater.*, **10**, 2561–2570.

McBirney, A.R., Aoki, K.I., Bass, M. (1967): Eclogites and jadeite from the Motagua fault zone, Guatemala. *Am. Mineral.*, **52**, 908–918.

Merlino, S. (1984): Feldspathoids: their average and real structures. *in* ''Feldspars and feldspathoids'', W.L. Brown, ed. D. Reidel Publishing Company, Dordrecht, 435–470.

Mitchell, A.H.G. (1993): Cretaceous-Cenozoic tectonic events in the western Myanmar (Burma)-Assam region. *J. Geol. Soc. London*, **150**, 1089–1102.

Miyajima, H., Matsubara, S., Miyawaki, R., Ito, K. (1999): Itoigawaite, a new mineral, the Sr analogue of lawsonite, in jadeitite from the Itoigawa–Ohmi District, central Japan. *Mineral. Mag.*, **63**, 909–916.

Miyajima, H., Matsubara, S., Miyawaki, R., Yokoyama, K., Hirokawa, K. (2001): Rengeite, $Sr_4ZrTi_4Si_4O_{22}$, a new mineral, the Sr–Zr analogue of perrierite from the Itoigawa–Ohmi district, Niigata Prefecture, central Japan. *Mineral. Mag.*, **65**, 111–120.

Morkovkina, V.F. (1960): Jadeitites in the hyperbasites of the Polar Urals. *Izv. Akad. Nauk Latv. SSR*, **4**, 78–82. (in Russian))

Nesse, W.D. (2000): Introduction to Mineralogy. Oxford University Press ed, London, 225 p.

Okay, A.I. (1997): Jadeite–K-feldspar rocks and jadeitites from northwest Turkey. *Mineral. Mag.*, **61**, 835–843.

Palmer, D.C. (1964): Stuffed derivatives of silica polymorphs. *Rev. Mineral.*, **29**, 83–122.

Ragimov, K.G., Chiragov, M.I., Mustafaev, N.M., Mamedov, Kh.S. (1978): Crystal structure of synthetic sodium-alumosilicate $Na_3Al_3Si_3O_{12}(H_2O)_2$. *Dok. Akad. Nauk SSSR*, **242**, 839–841.

Reinhardt, A., Hellner, E., Ahsbahs, H. (1982): Die Kristallstruktur von Nephelinhydrat I, einem Zeolith. *Fortsch. Mineral. Beiheft*, **60**, 175–176.

Roth, G. (1985): Zum Zusammenhang zwischen Ionenleitung und Kristallstruktur von Festkörperelektrolyten: theoretische Modelle sowie experimentelle Untersuchungen an Phasen des Nephelin Typs. PhD thesis, Universität Münster, Germany.

Schertl, H.-P., Maresch, W.V., Stanek, K.P., Hertwig, A., Krebs, M., Baese, R., Sergeev, S.S. (2012): New occurrences of jadeitite, jadeite quartzite and jadeite-lawsonite quartzite in the Dominican Republic, Hispaniola: petrological and geochronological overview. *Eur. J. Mineral.*, **24**, 199–216.

Seitz, R., Harlow, G.E., Sisson, V.B., Taube, K.E. (2001): Formative jades and expanded jade sources in Guatemala. *Antiquity*, **87**, 687–688.

Selker, P., Bartsch, H.H., Klaska, R. (1985): Struktur und Hydrothermalsynthesen von $NaAlSiO_4$ Modifikationen. *Z. Kristallogr.*, **170**, 175–176.

Shepelev, Y.F., Smolin, Y.I., Butikova, I.K., Tarasov, V.I. (1983): The crystal structure of zeolite Na Z-21 in hydrated and dehydrated states. *Dok. Akad. Nauk SSSR*, **272**, 1133–1137.

Shi, G.H., Cui, W.Y., Liu, J., Yu, H.X. (2001): The petrology of jadeite-bearing serpentinized peridotite and its country rocks from North-western Myanmar. *Acta Petrol. Sin.*, **17**, 483–490.

Shi, G.H., Cui, W.Y., Cao, S.H., Jiang, N., Jian, P., Liu, D.Y., Miao, L.C., Chu, B.B. (2008): Ion microprobe zircon U-Pb age and geochemistry of the Myanmar jadeitite. *J. Geol. Soc. London*, **165**, 221–234.

Shi, G.H., Jiang, N., Wang, Y., Zhao, X., Wang, X., Li, G., Ng, E., Cui, W. (2010): Ba minerals in clinopyroxene rocks from the Myanmar jadeitite area: implications for Ba recycling in subduction zones. *Eur. J. Mineral.*, **22**, 199–214.

Shi, G.H., Harlow, G.E., Wang, J., Wang, J., Ng, E., Wang, X., Cao, S., Cui, W.Y. (2012): Mineralogy of jadeitite and related rocks from Myanmar: a review with new data. *Eur. J. Mineral.*, **24**, 345–370.

Shigeno, M., Mori, Y., Shimada, K., Nishiyama, T. (2012): Jadeitites with metasomatic zoning from the Nishisonogi metamorphic rocks, western Japan: fluid–tectonic block interaction during exhumation. *Eur. J. Mineral.*, **24**, 289–311.

Swe, W. (1981): Tectonic evolution of the western ranges of Burma. *Contrib. Burmese Geol.*, **1**, 45–46.

Tsujimori, T. & Harlow, G.E. (2012): Petrogenetic relationships between jadeitite and associated high-pressure and low-temperature metamorphic rocks in worldwide jadeitite localities: a review. *Eur. J. Mineral.*, **24**, 371–390.

Vigny, C., Socquet, A., Rangin, C., Chamot-Rooke, N., Pubellier, M., Bouin, M.-N., Bertrand, G., Becker, M. (2003): Present day crustal deformation around Sagaing fault, Myanmar. *J. Geophys. Res.*, **108**, 2533.

Vulić, P., Kahlenberg, V., Konzett, J. (2008): On the existence of a Na-deficient monoclinic trinepheline with composition $Na_{7.85}Al_{7.85}Si_{8.15}O_{32}$. *Am. Mineral.*, **93**, 1072–1079.

Vulić, P., Kahlenberg, V., Gspan, C., Dimitrijević, R. (2013): Reinvestigation of pure Na-nepheline like compounds obtained from the thermal conversion of zeolite LTA. *Eur. J. Mineral.*, **25**, 473–478.

Yamada, H., Matsui, Y., Ito, E. (1983): Crystal-chemical characterisation of $NaAlSiO_4$ with the $CaFe_2O_4$ structure. *Mineral. Mag.*, **47**, 177–181.

Yui, T.F., Maki, K., Wang, K.L., Lan, C.Y., Usuki, T., Iizuka, Y., Wu, C.M., Wu, T.W., Nishiyama, T., Martens, U., Liou, J.G., Grove, M. (2012): Hf isotope and REE compositions of zircon from jadeitite (Tone, Japan, and north of the Motagua fault, Guatemala): implications on jadeitite genesis and possible protoliths. *Eur. J. Mineral.*, **24**, 263–275.

Received 4 September 2013
Modified version received 22 November 2013
Accepted 9 December 2013